Improving the Grain Growth model in the outer part of a circumstellar disc

Report ISIMA school 2011

ISIMA student: M. Galvagni
PI: Prof. P. Garaud
Collaborators: Dr. C. Olczak, Dr. F. Meru

Abstract

Observations of T-Tauri circumstellar discs show the presence of mm or cm size dust grains at large distances from the central star (r > 10s AU). There empirical data challenge the currently mainstream grain growth theory, that disfavours the formation of such large grains in the outer disc and, despite formation, predicts their rapid inward migration due to coupling with the gas on short timescales. In this work, we develop some improvements in the grain growth theory and implement them in GrOG (Growth Of Grains), a new numerical solver for the coagulation and fragmentation of grains inside a circumstellar disc. Our results revise conclusions from previous theoretical models, as we are able to growth particles of significantly larger size.

1 Introduction

Planets are born in the circumstellar discs typically found around young stars, which form from the collapse of a molecular cloud core. Circumstellar discs are made of two components: gas and dust. Observations have shown that in the outer parts of discs grain sizes can reach values as large as mm or even cm (see Wilner et al 2005). This is in contrast to theoretical predictions for the collisional growth of grains, which struggle to produce grains of this dimension at large distances. Furthermore, even if they grow to this size, they are rapidly lost due to the radial drift. This problem is

usually referred to as the mm size problem at 100 AU, similar to the more familiar meter size problem at 1 AU.

The evolution of the circumstellar disc is dominated by the gas, as this component dominates the total mass. The theory which describes the structure and evolution of gas discs was developed in 1974 by Lynden-Bell and Pringle; they derived the radial velocity of the gas u due to mass and angular momentum conservation inside a viscous disc with viscosity ν:

$$u(r) = -\frac{3}{\Sigma\sqrt{r}}\frac{\partial}{\partial r}\left(\Sigma\nu\sqrt{r}\right) \tag{1}$$

where r is the radius and Σ gas surface density. This quantity can be evaluated starting from the mass conservation equation and vertically integrating it:

$$\frac{\partial\Sigma}{\partial t} + \frac{1}{r}\frac{\partial}{\partial r}\left(r\Sigma u\right) = 0 \tag{2}$$

This equation admits self similar solutions of the kind

$$\Sigma(r,t) = \frac{M_{disk}}{2\pi r R_0 T^{3/2}}\exp\left(-r/R_0 T\right) \tag{3}$$

with M_{disk} is the initial disc mass, R_0 the initial disc radius, $T = t/\tau_\nu + 1$, where $\tau_\nu = R_0^2/3\nu_t(R_0)$ is the viscous spreading time (the viscosity is $\nu_t(r)$).

This concerns the evolution of the gas, but the disc has also a dust component. The behavior of the dust is related to that of the gas; the dust radial velocity v is

$$v = \left(u - 2\eta\tau\Omega\frac{\rho_0}{\rho}\right) / \left[1 + (\rho_0\tau\Omega/\rho)^2\right] \tag{4}$$

with ρ being the gas density, $\tau = (\rho(s)s) / (c\rho_0)$ the stopping time of the particle, with $\rho(s)$, s the density and size of the particle, c the local sound speed, $\rho_0 = 1g/cm^3$, $\Omega = \sqrt{(GM_{star})/r^3}$ the Keplerian frequency and $\eta = -\frac{c^2}{\Omega\rho}\frac{\partial\rho}{\partial r}$. The stopping time gives an idea of the influence of the gas pressure on the grains: if the size of the grain is small, or if the gas density is higher, the grain is strongly coupled with the gas, and they velocities are equal. As the particle grows, it starts decoupling from the gas, tries to settle into a Keplerian orbit, but then feels a head-on wind from the gas component as drifts inward. For larger particles, which are completely decoupled from the gas, follow a Keplerian orbit and do not drift.

Beside interacting with the gas, dust grains interact with each other through collisions. There are have three possible outcomes from these interactions: coagulation,

fragmentation or bouncing. The combination of all these encounters determines the evolution of the grain size distribution. Mathematically, these can be modeled by the standard Smoluchowski coagulation/fragmentation equations, which have the form:

$$\frac{dN_k}{dt} = \frac{1}{2}\sum_{i,j=1}^{k} C_{ijk}N_iN_j - \sum_{i}^{N}\sum_{j=k+1}^{N} C_{ikj}N_iN_k - \frac{1}{2}\sum_{i,j=1}^{N} F_{ikj}N_iN_k + \sum_{i,j=1}^{N} F_{ijk}N_iN_j \quad (5)$$

where N_k is the number of particle of mass m_k, C_{ijk} is the coagulation kernel, so the probability that particle i and j coagulate into particle k as a result of a collision and in a similar way F_{ijk} is the fragmentation kernel, so the probability that particle k forms as a fragment from the collision between particle i and j. The kernels are given by the number of collisions times the coagulation/fragmentation efficiency ϵ_i:

$$C_{ijk} = \sum_{i,j=1}^{k} N_iN_jm_im_j\Delta v(s_i,s_j)A(s_i,s_j)\epsilon_c \quad (6)$$

$$F_{ijk} = \sum_{i,j=1}^{N} N_iN_jm_im_j\Delta v(s_i,s_j)A(s_i,s_j)\epsilon_f \quad (7)$$

with $\Delta v(s_i, s_j)$ and $A(s_i, s_j)$ relative velocity and cross section for the collision between particle i and j. In this report, we present the results we obtained for the grain size evolution in the outer part of a T-Tauri disc using GrOG, a new coagulation-fragmentation code which is a simplified version of the code presented in Brauer et al. 2008 . In section 2 we present GrOG and the physics it implements; section 3 show our simulations and finally in section 4 we discuss our results and compare them with previous work.

2 Methods: GrOG

We present the new coagulation-fragmentation integrator GrOG (Growth Of Grains). This code solves the coagulation and fragmentation equation (5); we focused in particular on four ingredients: mass distribution of the grains with their size, cross section, relative velocity, coagulation and fragmentation probabilities. For all of these ingredients (except the cross section), GrOG implements more than one possible scheme. The details are given in the following sections.

2.1 Density distribution and cross section

It is usually assumed that the internal grains density is constant throughout the growth process, so that the mass of a particle is proportional to its size with the power law s^3. In contrast, laboratory experiments (see Blum and Wurm 2008, Ormel et al. 2011) show evidence of a *fractal growth*, resulting in a size-dependent density. Very small particles are compact, as they come from the interstellar medium; they start growing by coagulation, but since they just randomly stick one on top of one-other, the resulting grain has a higher porosity, where porosity can be quantified using the volume filling factor, defined as

$$\phi = \frac{\text{Volume occupied by N grains}}{\text{Volume equivalent to surface area}} \tag{8}$$

Beyond a certain size, collisions lead to compaction. The net effect of these processes is that the density is a complex function of the particle size. In GrOG we have thus two optional schemes: in the first, the density is kept constant (as it is usually done in this type of investigation). In the second scheme, internal density of grains is given by

$$\rho(m \leq m_{cr}) = \rho_{max} - \frac{\rho_{max} - \rho_{min}}{(m_{cr} - m_{min})^2}(m_{cr} - m)^2 \tag{9}$$

$$\rho(m > m_{cr}) = \rho_{max} \tag{10}$$

where ρ_{min} and ρ_{max} are respectively the density for the most porous and for the compact particle and m_{min} is the mass of the smaller particle. The critical mass between the two regimes m_{cr} is $\simeq 10^{-6}$g.

Interactions between particles are evaluated using the geometrical cross section:

$$A(s, s') = \pi(s + s')^2 \tag{11}$$

This assumption is consistent with our study of the outer region of the disc, where none of the particles are expected to growth so large as to require the inclusion of the gravitational cross section.

2.2 Relative velocity

There are four fundamental physical mechanisms that determine the velocity of dust particles: radial drift, turbulence, vertical settling and brownian motion. The dominant mechanism depends on the particle size (eg, brownian motion dominates the collisions of very small particles, while turbulence is most important if the grains

have very different sizes). For each pair of colliding particles, their relative velocity is given by the maximum of the four mechanisms.

For radial drift, which is the velocity that the particle acquires via its coupling with the gas, the relative velocity is the difference between the velocities given by Eq. 4. Adopting the initial parameters of the disc that will be presented in Sec. 3.1, the radial drift velocity for a particle of size s is

$$v(s) = \frac{u_{gas} - 2\eta B}{1 + B^2} \tag{12}$$

with

$$\eta = \frac{9}{4} h_0^2 \sqrt{\frac{GM_{star}}{1AU}} \tag{13}$$

$$B = \rho_s s (2\pi)^{(3/2)} \frac{R_0 r}{M_{disk}} \tag{14}$$

where all the parameters are defined as in 3.1.

The relative velocities of particles induced by their interactions with turbulent eddies were calculated by Ormel and Cuzzi 2007, and depends on the ratio of the particle stopping time with the eddy turnover time:

$$\left[\frac{[\tau(s) - \tau(s')]^2}{\tau_d[\tau(s) - \tau(s')]}\right]^{1/2} v_e \text{ if } \tau(s),\tau(s') \leq \tau_\nu \tag{15}$$

$$v_e \text{ if } \tau(s') \leq \tau_d \leq \tau(s) \tag{16}$$

$$\left[\frac{\tau_d}{\tau_d + \tau(s)} + \frac{\tau_d}{\tau_d + \tau(s')}\right] v_e \text{ if } \tau_d \leq \tau(s), \tau(s') \tag{17}$$

$$\frac{3}{\tau(s) + \tau(s')} \left(\frac{max(\tau(s), \tau(s'))}{\tau_d}\right)^{1/2} v_e \text{ otherwise} \tag{18}$$

where $v_e \simeq \sqrt{\alpha} c$ is the velocity for the smaller eddy, $\tau_d = \sqrt{GM(<r)/r^3}$ is the dynamical timescale of the disc and $\tau_\nu = \tau_d Re^{-1}$ is the dissipation timescale of the disc, with $Re \simeq 10^{14}$ Reynold number for a viscous disc. Heuristically, this can be interpreted in the following way: the first case corresponds to two small particles both being trapped within the smallest eddy, so very affected by the turbulence. In the second case, one of the particle is larger and its motion is still affected by the eddies, but not longer dominated by them, while the second particle is. In the third case, both particles have large enough stopping times to be just slightly influenced by the turbulence. The fourth case covers all the other possibilities (eg, one particle is no longer inside the smaller eddy, but has not decoupled yet from the turbulence).

The vertical settling velocity describes the velocity acquired by the particles that are above the midplane while they fall on it. In this case we adopt the same scheme as in Birnstiel (2011):

$$v_S(s) = \min(0.5, \tau(s)/\tau_d) h(r) \min\left(1.0, \sqrt{\frac{\alpha}{(1+(\tau(s)/\tau_d)^2)\min(0.5, \tau(s)/\tau_d)}}\right) \Omega \tag{19}$$

where Ω is the Keplerian angular velocity. The relative settling velocity is simply $v_S(s) - v_S(s')$.

The brownian motion gives relative velocities:

$$\Delta v_B(s, s') = \sqrt{8 k_B \frac{m(s) + m(s')}{\pi m(s) m(s')}} \tag{20}$$

where k_B is the Boltzmann constant.

Using these equations, we visualize the relative collision velocity of two particles over a range of sizes. Our result is presented in Fig. 1 and recovers the work of Brauer et al. 2008.

2.3 Coagulation and fragmentation efficiency

A number of laboratory experiments have been run to determine which is the dominant outcome (fragmentation, coagulation or bouncing) of a collision between two particles given their sizes and relative velocity (Blum 2010, Blum and Wurm 2008). Unfortunately, usually silicate grains are used in these experiments, while in the outer part of circumstellar disc , which is the region we are interested in, the grains are mainly composed by ices. There exist only a few experiments and models in this contest, among which the collisional fusion model of Wettlaufer (2011), which seems to be promising and will need to be taken into account in future studies.

The results of these experiments have been recently implemented in numerical models simulating the evolution of the grain size distribution in a circumstellar disc has been developed. In this report we will call "Brauer model" the one implemented in Brauer et al (2008) and we will use it as a reference. This scheme includes only fragmentation and coagulation, but ignores cratering. Given a critical fragmentation velocity $v_f = 30$ m/s, the fragmentation efficiency ϵ_f is

$$\epsilon_f(\Delta v) = \left(\frac{\Delta v}{v_f}\right)^{\psi} \Theta(vf - \Delta v) + \Theta(\Delta v - vf) \tag{21}$$

with $\psi = 1$ and Θ Heaviside step function. If fragmentation happens, the total mass of the two colliding grains is redistribuited following the mass distribution function

$$n(m)dm \propto m^{-\epsilon}dm \tag{22}$$

where usually $\epsilon = 1.83$, as given by laboratory experiments (Mathis et al. 1977, Draine and Lee 1984). The coagulation probability in this scheme is $\epsilon_c = 1 - \epsilon_f$. Fig. 2 shows the coagulation and fragmentation probabilities given a critical fragmentation velocity $v_f = 30$ m/s. Note that for relative velocities larger than the critical value, the coagulation probability is always zero. This means that once the particles have grown large enough that collisional velocities are always longer than that threshold, it is impossible for them to grow further and only fragmentation can happen. Effectively, there is a maximal size that particles can not overcome, called the "fragmentation barrier", as it has been pointed out in Birnstiel (2011).

However, we have also implemented another more realistic coagulation and fragmentation scheme in GrOG, here called the "Tail model". In this scheme we assume that the fragmentation probability function is a step function, with value 1 for relative velocities larger than v_f and 0 in the other case. We take into account that the relative velocity of colliding particles is not fixed by Eq. 12 - 20, but follows a Maxwellian distribution centered on the value determined by these equations. By making the convolution of this two functions, we obtain that the fragmentation efficiency is

$$\epsilon_f = \exp\left(-v_f/(2\sigma_f)\right)^2 + \frac{v_f^2}{4\sigma_f^2}\exp\left(-v_f/(2\sigma_f)^2\right) \tag{23}$$

with $\sigma_f = \sqrt{\pi}\Delta v/4$. In analogy, we define the coagulation probability to be 1 for relative velocities smaller than a critical value v_c and 0 otherwise and following the same procedure, the coagulation efficiency is

$$\epsilon_c = \exp\left(-v_c/(2\sigma_c)\right)^2 + \frac{1}{4\sigma_c^2}\exp\left(-v_c/(2\sigma_c)\right)^2(v_c)^2 \tag{24}$$

with $\sigma_c = \sqrt{\pi}\Delta v/4$. Note that in this scheme the coagulation efficiency is never zero, and for large velocities behaves like $\propto \Delta v^{-4}$; this implies that there is no theoretical maximum size for successful coagulation - only the probability gets very low -. Note also that, if onte assumes $v_f = v_c$, then $\epsilon_f + \epsilon_c = 1$; if instead $v_c < v_f$ there is a region where $\epsilon_f + \epsilon_c < 1$ which naturally defines a bouncing region. In figure 3 we show the coagulation and fragmentation efficiency for the Tail model with and without bouncing.

Finally recent laboratory experiments (see the review by Blum, 2010) show that collision of porous dust aggregates on compact objects reveal a second sticking regime

Tab. 1: Simulations

Sim	Model	Porosity	v_c [m/s]	v_f [m/s]	II Sticking regime
A	Brauer	No	30.0	30.0	NO
B	Brauer	$\rho_{min} = 0.1$ g/cm^3	30.0	30.0	NO
C	Brauer	$\rho_{min} = 0.01$ g/cm^3	30.0	30.0	NO
D	Brauer	NO	30.0	30.0	$s_c = 10$
E	Tail	NO	30.0	30.0	NO
F	Tail	$\rho_{min} = 0.1$ g/cm^3	30.0	30.0	NO
G	Tail	$\rho_{min} = 0.01$ g/cm^3	30.0	30.0	NO
H	Tail	NO	30.0	50.0	NO
I	Tail	NO	30.0	100.0	NO
L	Tail	NO	30.0	30.0	$s_c = 10$

beyond the bouncing region (in velocity space), so that in high-velocity encounters fragmentation doesn't occur. We have implemented this scenario into the Tail model. Because in our model only large particles can become compact, for size ratios larger than a critical value s_c the coagulation efficiency is set to one.

In Fig. 4 we compare the coagulation efficiencies that are determined implementing the different models presented in this section.

3 Results

This section presents the results of our simulations based on GrOG. We studied the evolution of the grain size distribution at $r = 100$ AU for a T-Tauri disc using different coagulation-fragmentation schemes. Table 1 summarizes the parameters for the simulations presented.

3.1 Initial conditions

The initial grain size distribution is assumed to be a Gaussian centered on $s = 10\mu$m. The circumstellar disc is assumed, for simplicity, to have a surface density profile constant in time and with a radial dependence:

$$\Sigma(r) = \frac{M_{disk}}{2\pi R_0 r} \tag{25}$$

Here we focus on the outer disc at $r = 100$ AU. Our disc parameters are those observationally determined for the TW Hydrae disc:

$$M_{\text{star}} = 0.8M_{\odot} \quad (26)$$
$$M_{\text{disk}} = 0.1M_{\text{star}} \quad (27)$$
$$R_0 = 200\text{AU} \quad (28)$$
$$\alpha = 0.01 \quad (29)$$
$$\text{Re} = 10^{14} \quad (30)$$
$$h(r = 100AU) = 10\text{AU} \quad (31)$$
$$\text{gas to dust ratio} = 0.01 \quad (32)$$
$$\rho_{max} = 1\text{g/cm}^3 \quad (33)$$
$$m_{cr} = 4 \times 10^{-6}\text{g} \quad (34)$$

3.2 Brauer Model

Simulations from A to D implement the Brauer model. In all these cases we assume that fragmenting and coagulation critical velocities are the same, and have value 30 m/s. This value is taken from Brauer et al. (2008), for case of comparison. When the porosity is implemented, the maximal density is assumed to be $\rho_{max} = 1$ g/cm^3, while the minimum value changes in simulations B and C (see table) by respectively one or two order of magnitude. In the last simulation (case D), we implement the second sticking region, assuming as the size ratio threshold $s_c = 10$. The results for the grain size evolution are presented in figure 5.

3.3 Tail Model

Simulations from E to L implement different versions of the Tail model. In the simplest configuration (set E), there is no porosity nor bouncing nor second sticking regime. The influence of the porosity is studied in simulations F and G, for two different values of the minimum density. Simulations H and I introduce the bouncing regime by increasing the critical fragmenting velocity. Last, case L implement the second sticking regime. The results are shown in figure 6.

4 Discussion and Future Work

The results for the Brauer model simulations are in agreement with what has been found before: the size distribution reaches an equilibrium state quite fast (in our

case, less than 10^4 yrs), with a maximum size that can't be overcome. Including the porosity increases this maximum size, although its value is still an order of magnitude smaller than the mm-size. This situation is solved by the inclusion of the second sticking regime.

The introduction of the Tail model changes in a significative way the outcome of the grain size distribution. Please note that the results presented herein are evolved for a maximal time $t = 3.5 \times 10^4$ yrs, as these simulations are computationally more time demanding. The first effect of this new model is that it is possible to overcome the maximum size: comparing simulation A and E indeed shows that in the latter case the evolution doesn't freeze for long time. This leads to the formation of larger grains, up to 0.5 mm. The introduction of the grains porosity (simulations F and G, see Tab 1 for details) doesn't help the formation of larger size particles, but leads to the formation of a depleted part in the size distribution around $s = 0.01$ cm. Implementation of the bouncing region in simulation H has no effect (compare with simulation E), but if we expand this region (simulation I) it is possible to see that this helps the very small grains (size less than 0.001 cm) to coagulate in larger particles. This is not a linear effect; what is supposed to be happening is that the presence of the bouncing stops the medium-size particles from growing, giving more time to the small ones to coagulate on them. Last, simulation L shows the effects of considering a second sticking regime. Also in this scenario, the net outcome is that the small grains are helped to coagulate, as they don't cause fragmentation any more when they encounter a large grain.

Our work presents the results for the evolution of the grain size distribution of particles for the outer part of a circumstellar disc using a new code, GrOG. We were able to reproduce previous results, and we also presented some improvements in the physical model for coagulation and fragmentation, the Tail model. Note that, although the implementation of this new model leads to the formation of larger size particles, we still don't observe mm or cm size objects, as detected in real discs. It is expected that by running these simulations for longer times we will be able to form them. In the future, there are still some aspects that need to be improved inside this code, as the turbulence model used for deriving the relative velocities, the porosity description, that needs to be more realistic, a physically meaningful evaluation of the critical velocities using the collisional fusion model.

Bibliography

- Blum J., 2010, Research in Astronomy and Astrophysics, Volume 10, Issue 12, pp. 1199-1214
- Blum J. & Wurm G., 2008, Annual Review Astro. Astrophys. 46:21-56
- Birnstiel 2011, PhD Thesis
- Brauer F., Dullemond C., Henning T. 2008, A & A 480, 859-877
- Draine B. T., Lee H. M. 1984, ApJ, 285, 89
- Mathis J. S., Rumpl W., Nordsieck K. H. 1977, ApJ, 217, 425
- Lynden-Bell, D. & Pringle, J. E. 1974, MNRAS, 168, 603
- Ormel C. W., Cuzzi J. N. 2007, A & A 466, 413
- Ormel C. W., Min M., Tielens A. G. G. M., Dominik C., Paszun D., 2011, A & A, 532, A43
- Wettlaufer J. S. 2011, The Astrophysical Journal, 719:540
- Wilner D. J., D'Alessio P., Calvet N., Claussen M. J. and Hartmann L. 2005, APJ, 626:L109-112

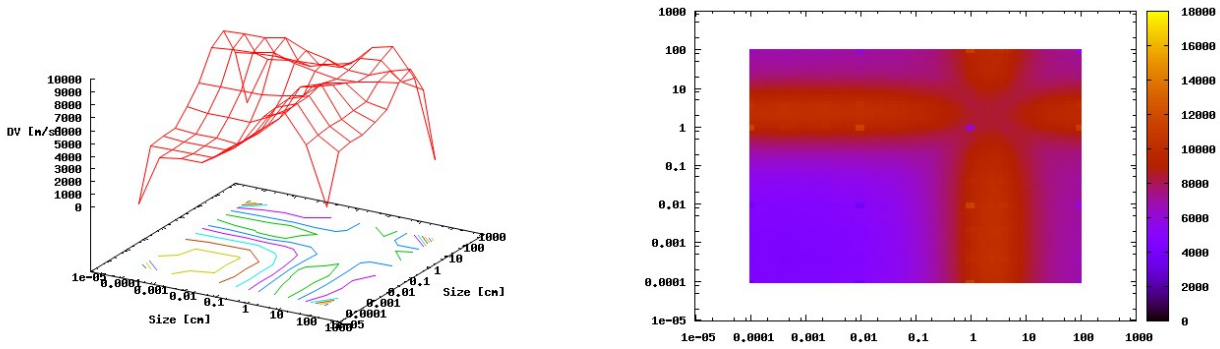

Fig. 1: Relative velocity as a function of the size of the colliding particles. On the left there is a 3D plot; on the right a 2D map. All the units are in cgs.

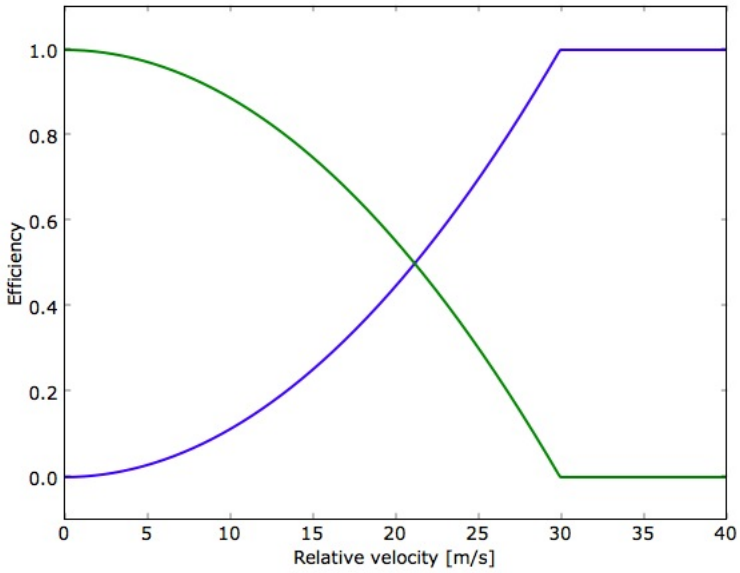

Fig. 2: Coagulation (in green) and fragmentation (in blue) efficiency as a function of relative velocity in the Brauer model, assuming $v_f = 30$ m/s.

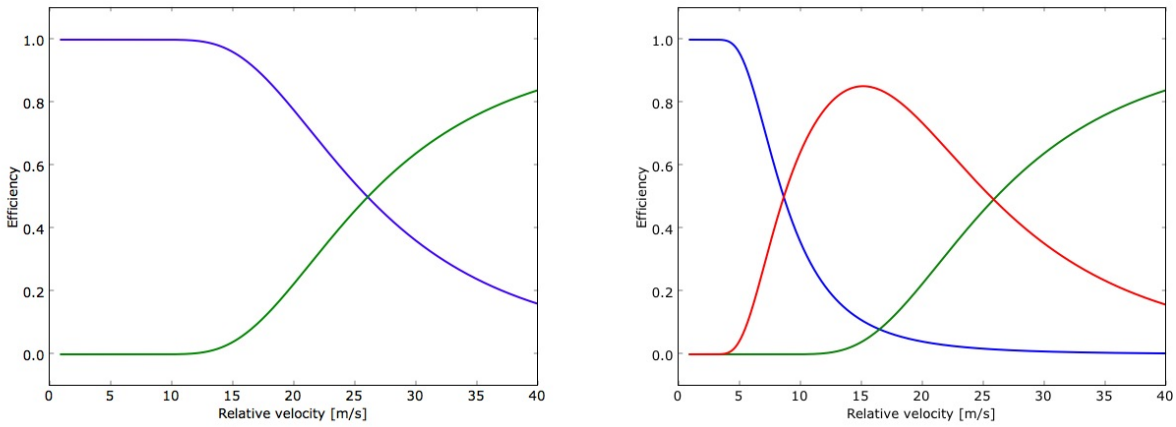

Fig. 3: Coagulation (in green) and fragmentation (in blue) efficiency as a function of relative velocity in the Tail model. On the left, the critical velocities are $v_f = v_c = 30$ m/s; on the right, $v_f = 30$ m/s and $v_c = 10$ m/s, so there is a bouncing region, whose probability is represented by the red line.

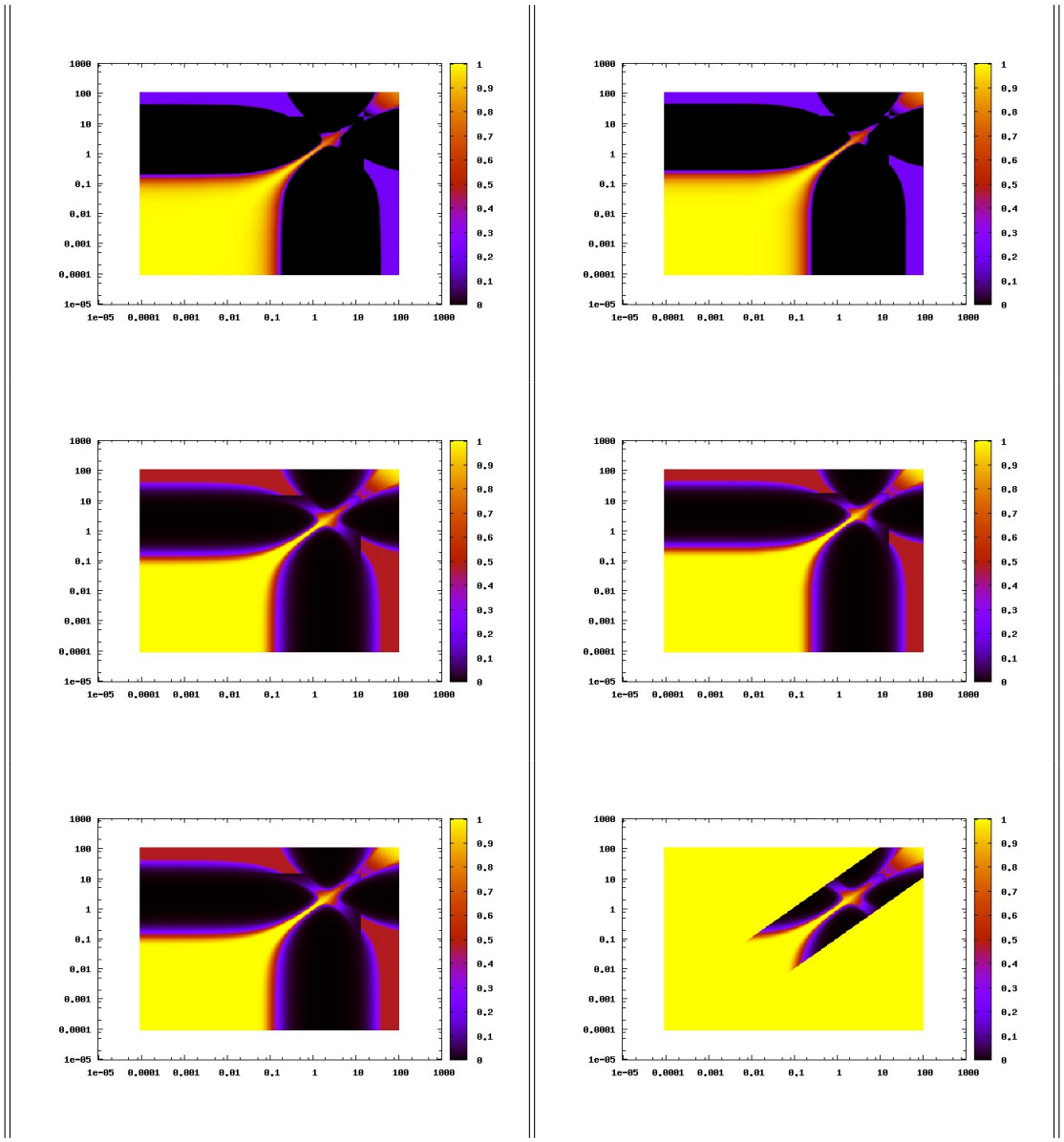

Fig. 4: Coagulation efficiency for the different models that are implemented in GrOG as a function of the particle size (in cm). From top to botton, from left to right: Brauer model, Brauer + porosity ($\rho_{\min} = 10^{-2}$ g/cm^3), Tail model, Tail + porosity, Tail + bouncing ($v_c = 30$ m/s and $v_f = 50$ m/s), Tail + second sticking regime (size ratio = 10).

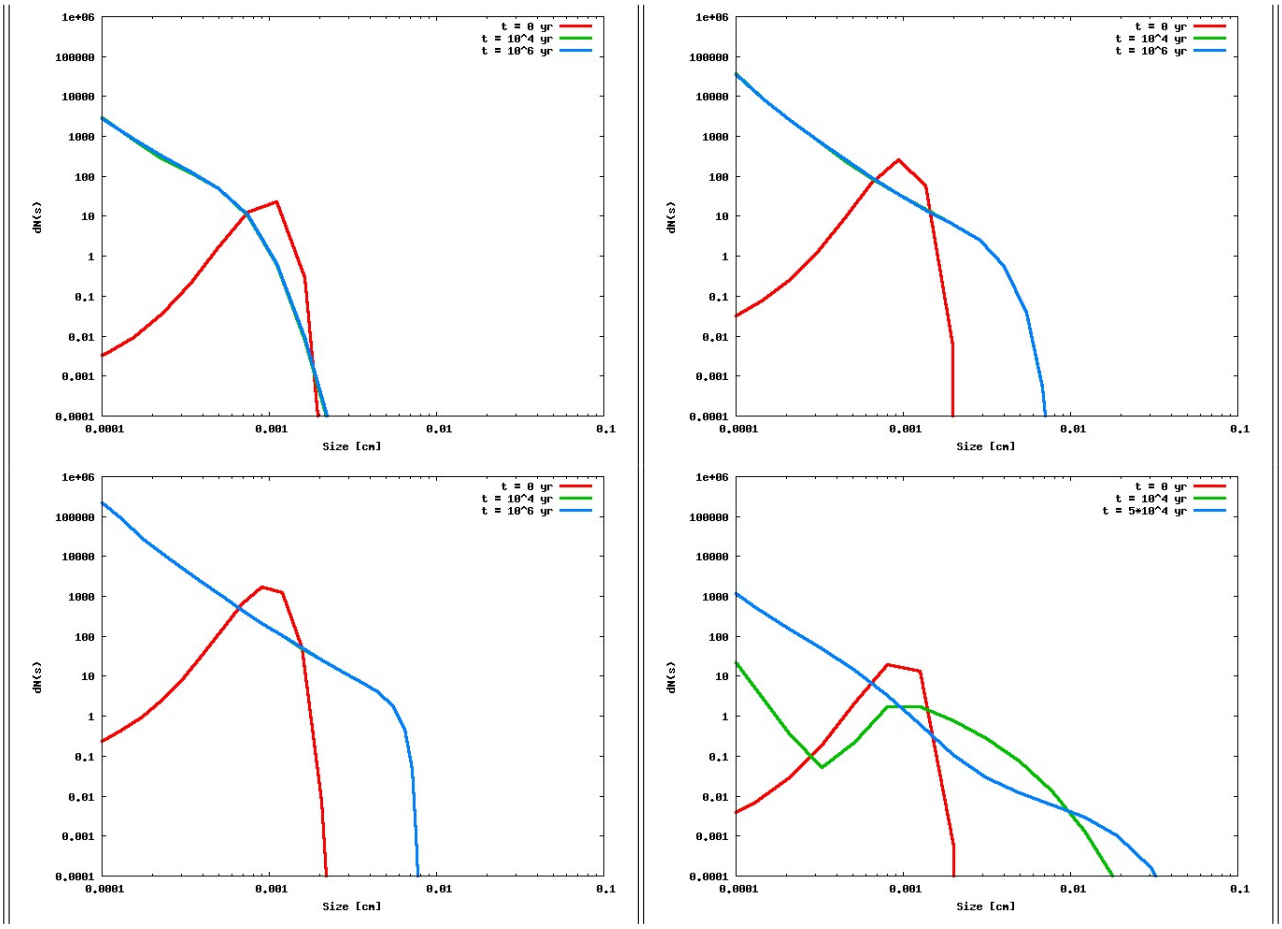

Fig. 5: Evolution of the grain size distribution. dN(s) is the number of particle inside a box of radius $a = 0.001$ au. From top to bottom, from left to right: simulation A, B, C and D.

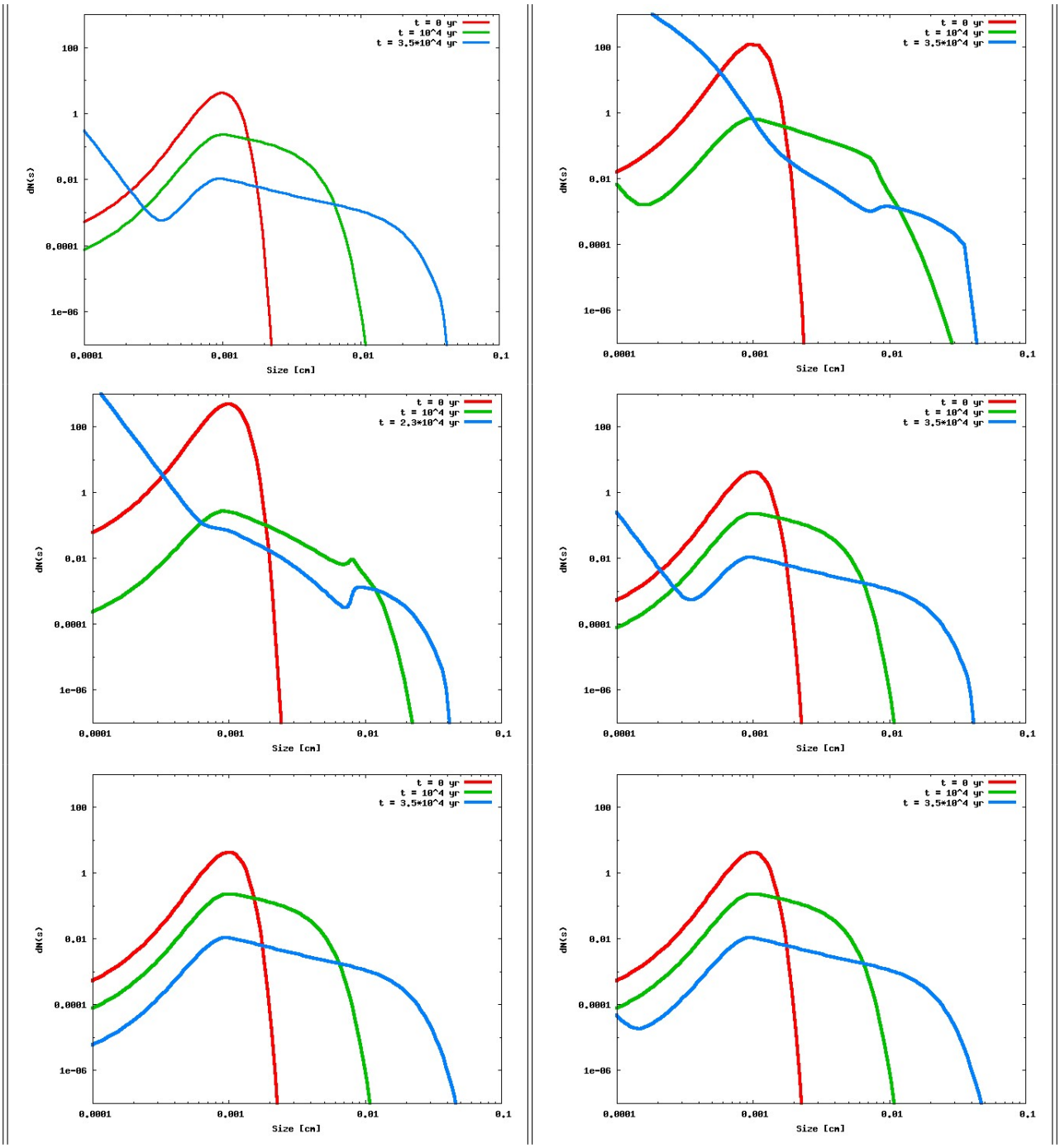

Fig. 6: Evolution of the grain size distribution. dN(s) is the number of particle inside a box of radius $a = 0.001$ au. From top to bottom, from left to right: simulation E, F, G, H, I and L.